Atmos. Chem. Phys., 11, 10243–10257, 2011
www.atmos-chem-phys.net/11/10243/2011/
doi:10.5194/acp-11-10243-2011

Atmospheric Chemistry and Physics

Acetylene C_2H_2 retrievals from MIPAS data and regions of enhanced upper tropospheric concentrations in August 2003

R. J. Parker, J. J. Remedios, D. P. Moore, and V. P. Kanawade

Earth Observation Science, Space Research Centre, University of Leicester, Leicester, UK

Received: 11 August 2010 – Published in Atmos. Chem. Phys. Discuss.: 7 December 2010
Revised: 28 September 2011 – Accepted: 29 September 2011 – Published: 13 October 2011

Abstract. Acetylene (C_2H_2) volume mixing ratios (VMRs) have been successfully retrieved from the Michelson Interferometer for Passive Atmospheric Sounding (MIPAS) Level 1B radiances during August 2003, providing the first global map of such data and ratios to CO in the literature. The data presented here contain most information between 300 hPa and 100 hPa with systematic errors less than 10 % at the upper levels. Random errors per point are less than 15 % at lower levels and are closer to 30 % at 100 hPa.

Global distributions of the C_2H_2 and C_2H_2/CO ratio confirm significant features associated with both the Asian monsoon anticyclone and biomass burning for this important hydrocarbon in a characteristic summer month (August 2003), showing tight correlations regionally, particularly at lower to medium values, but globally emphasising the differences between sources and lifetimes of CO and C_2H_2. The correlations are seen to be particularly disturbed in the regions of highest C_2H_2 concentrations, indicating variability in the surface emissions or fast processing.

A strong isolation of C_2H_2 within the Asian monsoon anticyclone is observed, evidencing convective transport into the upper troposphere, horizontal advection within the anticyclone at 200 hPa, distinct gradients at the westward edge of the vortex and formation of a secondary dynamical feature from the eastward extension of the anticyclone outflow over the Asian Pacific. Ratios of C_2H_2/CO are consistent with the evidence from the cross-sections that the C_2H_2 is uplifted rapidly in convection.

Observations are presented of enhanced C_2H_2 associated with the injection from biomass burning into the upper troposphere and the outflow from Africa at 200 hPa into both the Atlantic and Indian Oceans. In the biomass burning regions, C_2H_2 and CO are well correlated, but the uplift is less marked and peaks at lower altitudes compared to the strong effects observed in the Asian monsoon anticyclone. Ratios of C_2H_2/CO clearly decay along transport pathways for the outflow, indicating photochemical ageing of the plumes.

Overall, the data show the distinctive nature of C_2H_2 distributions, confirm in greater detail than previously possible features of hydrocarbon enhancements in the upper troposphere and highlight the future use of MIPAS hydrocarbon data for testing model transport and OH decay regimes in the middle to upper troposphere.

Correspondence to: R. J. Parker
(rjp23@le.ac.uk)

1 Introduction

The burning of vegetation, both living and dead, can release large quantities of gases into the atmosphere. Biomass burning is therefore a major source for the injection of trace gases into the atmosphere. Biomass burning and combustion were thought to be the major sources of acetylene (C_2H_2) (Hegg et al., 1990; Blake et al., 1996; Whitby and Altwicker, 1978). However, recent work proposes biofuel emissions as the dominant source with Xiao et al. (2007) estimating that as much as half of global C_2H_2 is biofuel-related ($3.3\,Tg\,yr^{-1}$) with the remainder due to fossil fuel ($1.7\,Tg\,yr^{-1}$) and biomass burning ($1.6\,Tg\,yr^{-1}$). Streets et al. (2003) found that 45% of the C_2H_2 emissions in Asia were due to biofuel. Streets et al. (2003) make a clear distinction between open biomass burning (i.e. forest fires) and the combustion of biofuels (wood, crop residue, dung, etc.) in domestic cooking and heating. The importance of biofuel as a C_2H_2 source has also been identified in Africa where the emission of C_2H_2 due to biofuel was significantly greater than that due to savannah biomass burning (Bertschi et al., 2003).

It is estimated that Asia accounts for around 70 % of global biofuel emissions as well as being a significant source for biomass burning and industrial emissions. Africa is also

a significant source of C_2H_2 emissions, whether through biomass burning, fossil fuel or biofuel emissions. The work presented here is intended to confirm the large C_2H_2 concentrations emanating from these regions.

The concentration of C_2H_2 is strongly correlated to CO and the C_2H_2/CO ratio can act as an indicator for source emissions and as a robust tracer for the photochemical evolution of the air mass since it last encountered a combustion source (Xiao et al., 2007). This allows an estimation of the relative photochemical age of biomass plumes and the amount of photochemical processing that the plume has undergone.

In addition to the interest in C_2H_2 as a tracer for the transport of biomass/biofuel burning, C_2H_2 plays an important role in the formation of glyoxal (CHOCHO) with implications for the production of secondary organic aerosol (SOA) (Volkamer et al., 2009). Hence, the ability to retrieve global distributions of C_2H_2 may also prove important for future air quality and climate simulations.

Whilst vertical profiles of C_2H_2 have been observed from aircraft measurements (Smyth et al., 1996; Talbot et al., 2003) and more recently from satellite observations (Rinsland et al., 2005), there is still some uncertainty as to the distribution of C_2H_2 due to the poor understanding of the emissions from the large number of varying sources (Streets et al., 2003). Recent work by Park et al. (2008) has observed enhancements of C_2H_2 inside the Asian monsoon anticyclone from space with the Atmospheric Chemistry Experiment (ACE-FTS) FTIR instrument (Bernath et al., 2005). Due to the solar occultation technique used there are relatively few observations over the tropical region, with the majority of ACE-FTS observations occurring at polar latitudes. This sparse spatial sampling makes it necessary, particularly in the tropics, to average occultation data over multiple months and years, making it less well-suited when studying dynamical events on short time-scales. Park et al. (2008) were able to find only ∼40 ACE-FTS profiles within the anticyclone between June and August over over 3 years (2004 to 2006).

In the present work, we wished to develop a new global set of observations, with which to overcome these problems, using infrared limb emission spectra for the upper troposphere recorded with the Michelson Interferometer for Passive Atmospheric Sounding (MIPAS). These provide greater temporal and spatial resolution than the ACE-FTS instrument albeit with a lower signal to noise ratio (SNR) per individual profile compared to the solar occultation method employed by ACE-FTS. Despite the higher noise on an individual profile, it was expected that good quality, high spatial resolution, distributions of C_2H_2 could be successfully determined on a per profile basis. Given the importance of the Asian monsoon anticyclone and biomass burning, the second objective of this work was to produce the first global map of C_2H_2, focusing on August 2003 where both effects could be observed. This would demonstrate both the quality of the data and provide useful information on the morphology of C_2H_2 which has not previously been observed in such great detail globally.

2 The MIPAS instrument

MIPAS is a core instrument onboard the ENVIronmental SATellite (ENVISAT) Satellite launched in March 2002. Measurements are performed by mid-infrared limb emission sounding of the atmosphere with a nominal mode (March 2002–March 2004) of 17 tangent altitudes with a vertical resolution of 3 km in the upper troposphere. MIPAS is a Fourier transform infrared spectrometer with a 0.025 cm^{-1} unapodised spectral resolution and measures over a large spectral range, from 685 cm^{-1} to 2410 cm^{-1}, observing the region of the atmospheric spectrum where there are a variety of molecules with vibration-rotation bands with well-defined absorption lines (Fischer et al., 2008). MIPAS is able to detect a wide range of trace species and is operationally used to retrieve pressure, temperature, O_3, H_2O, CH_4, HNO_3, N_2O and NO_2 from 6 to 68 km (Raspollini et al., 2006). Various non-operational trace species have been detected and retrieved from MIPAS spectra including PAN (Moore and Remedios, 2010; Glatthor et al., 2007), HCFC-22 (Moore and Remedios, 2008) and C_2H_6 (von Clarmann et al., 2007).

This work utilises the full resolution Level 1B (L1B) MIPAS spectra from August 2003 with the instrument measuring at 17 vertical levels and an unapodised spectral resolution of 0.025 cm^{-1} before technical issues resulted in a reduction in resolution to 0.0625 cm^{-1} after August 2004.

3 Determination of C_2H_2 in the upper troposphere

The objective of the retrieval work was to examine the C_2H_2 spectral signatures in MIPAS L1B spectra with a full optimal estimation retrieval algorithm in order to identify regions of high C_2H_2 volume mixing ratios (VMRs). Due to the high spatial sampling of the MIPAS instrument, such retrievals allow global sampling of dynamical events at relevant timescales, of particular relevance to regions of biomass burning and deep convection such as the Asian Monsoon anticyclone.

The spectral window used for this work is outlined in Fig. 1 where the contributions from each species to the total radiance (black) are shown. The Oxford Reference Forward Model (RFM) (Dudhia, 2005b) was used to model the spectra as observed by MIPAS. The RFM is a line-by-line radiative transfer model based on the GENLN2 model (Edwards, 1992). The spectroscopic information is taken from the HITRAN2004 spectral database (Rothman et al., 2005; Jacquemart et al., 2003) and in this case the simulation uses a standard atmospheric climatology (Remedios et al., 2007) with an enhancement of the C_2H_2 profile typical of biomass burning taken from Rinsland et al. (2005).

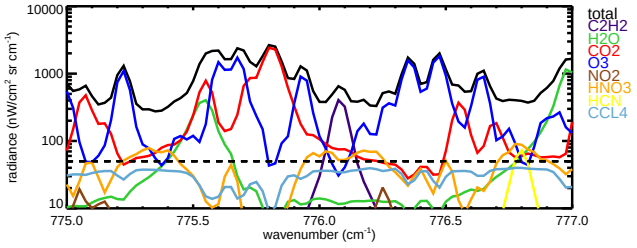

Fig. 1. RFM simulation of a 12 km MIPAS spectra at a 0.025 cm^{-1} resolution covering a 2 cm^{-1} range around the prominent C_2H_2 feature at 776.075 cm^{-1}. This shows the contribution to the C_2H_2 microwindow (776.0 cm^{-1} to 776.15 cm^{-1}) from interfering species and uses a standard atmosphere background with an enhanced C_2H_2 profile typical of biomass burning observations. These contributions are defined as the difference between the total simulated radiance and the simulated radiance when the contributing gas has been omitted from the calculation.

In Fig. 1, one line of the ν_5 band of C_2H_2 (purple line) can be seen to be the dominant feature in the 776.0 cm^{-1} to 776.15 cm^{-1} spectral range and unlike other C_2H_2 spectral lines in this region at 755 cm^{-1}, 762 cm^{-1} and 766.7 cm^{-1} the line is not masked by a strong ozone feature (Rinsland et al., 1998). This clear spectral line allows the unambiguous identification of enhanced C_2H_2 in MIPAS L1B spectra in this microwindow.

3.1 Retrieval method

A full optimal estimation approach was taken to retrieve the C_2H_2 VMR. The MIPAS Orbital Retrieval using Sequential Estimation or MORSE (Dudhia, 2005a) scheme is an optimal estimation scheme developed by the University of Oxford based on the approach taken by Rodgers (2000) and has recently been used to successfully retrieve peroxyacetyl nitrate (PAN) from MIPAS observations by Moore and Remedios (2010) where further details of the retrieval scheme are provided.

The MORSE approach involves the inversion of the measured spectral radiances ($\boldsymbol{y}$) in order to obtain the best solution for the retrieved parameters (the state vector $\boldsymbol{x}$) with the associated random error, $\boldsymbol{\epsilon}$. The relationship between the retrieved parameters and the measured radiances is defined by a forward model $\mathbf{F}(x)$, in this case the RFM, which performs the radiative transfer calculations to calculate the expected radiance given the input parameters. The retrieval is performed sequentially, layer by layer.

As described by Rodgers (2000), the solution to the above is constrained with respect to the a priori information (in this case standard climatologies) by the a priori covariance and the solution is found by minimising the cost function χ^2 via an iterative procedure where the state vector ($\boldsymbol{x}$) is updated after each iteration.

This iterative procedure for the state vector is

$$\boldsymbol{x}_{i+1} = \boldsymbol{x}_i - (\mathbf{S}_\mathbf{a}^{-1} + \mathbf{K}_i^T \mathbf{S}_y^{-1} \mathbf{K}_i + \gamma \mathbf{D})^{-1} \quad (1)$$
$$(-\mathbf{K}_i^T \mathbf{S}_y^{-1}[\boldsymbol{y} - \mathbf{F}(\boldsymbol{x}_i)] + \mathbf{S}_\mathrm{a}^{-1}[\boldsymbol{x}_i - \boldsymbol{x}_\mathrm{a}])$$

where $\mathbf{K}$ is the Jacobian matrix, $\boldsymbol{x}_\mathrm{a}$ is the a priori value and $\mathbf{D}$ is the scaling matrix. $\mathbf{S}_\mathrm{a}$ is the a priori covariance matrix where diagonal values equivalent to a 1000 % standard deviation of the C_2H_2 VMR along with a correlation length (off-diagonal decay of covariance with altitude) of 3 km were necessary to account for the large variations in VMR over biomass burning regions. $\mathbf{S}_y$ is the measurement error covariance and was taken to be equivalent to a conservative estimate of the MIPAS spectral noise in Band A of 40 nW/(cm^2 sr cm^{-1}) (Fischer et al., 2008); note that the noise in apodised spectra can reduce to lower than 20 nW/(cm^2 sr cm^{-1}).

The reduction of the cost function at each iteration is used to test for convergence and the final value is useful in determining whether the obtained solution is a sensible value. Ideally, the value for $\boldsymbol{\chi}^2$ should be equal to the number of degrees of freedom in the retrieval.

In order to accurately retrieve C_2H_2 it was necessary to obtain accurate VMRs of the other interfering species in the spectral range. Therefore, prior to retrieving C_2H_2, MORSE was used to retrieve profiles of pressure/temperature, H_2O, O_3 and HNO_3 respectively which were subsequently used as a priori for the C_2H_2 retrievals. The sensitivity of the retrieval to these species is examined in Sect. 3.3.

3.2 Retrieval setup

C_2H_2 VMRs were retrieved for August 2003 for the 9 km to 30 km nominal MIPAS altitudes. The results presented in this paper are primarily for the upper-tropospheric limb measurements at a 12 km nominal altitude with a corresponding average pressure of 200 hPa. The retrieval used MORSE L1C files which were created by extracting radiance information for the C_2H_2 microwindow from the MIPAS L1B spectra and applying a Norton-Beer Medium apodisation. Only retrieved data where the cloud index (Spang et al., 2004) was greater than 4.0 (corresponding to clear-sky conditions) and the normalised χ^2 value was less than 2.0 were used. It was also confirmed that there were only small differences between the measured and simulated spectra, with maximum values less than 40 nW/(cm^2 sr cm^{-1}), consistent with MIPAS measurement noise.

3.3 Error analysis

Figure 2 shows the final errors calculated for the retrieval, showing the total calculated error (solid line), the random component (dotted line) and the systematic component (dashed line). The systematic model parameter errors shown for each variable are 1σ values calculated from measured biases in the MIPAS data and were taken from

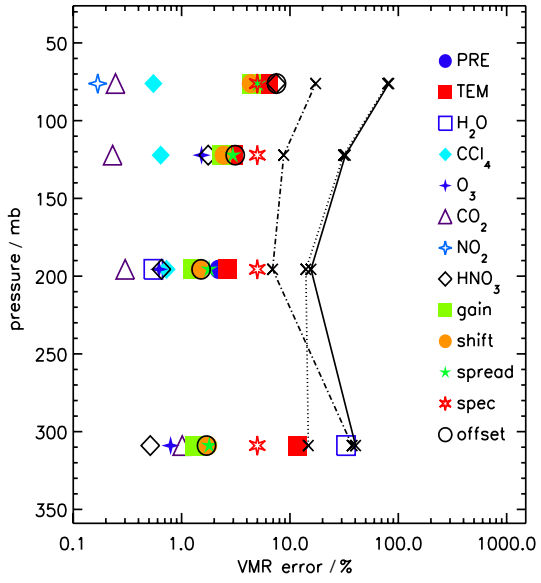

Fig. 2. Contributions to the C_2H_2 retrieval error. The total error (solid line), random error (dotted line) and the systematic error (dashed line) are all shown as well as the various components to the systematic error such as the Instrument Line Shape and spectroscopic errors.

Fischer et al. (2008). Uncertainties of 2 % were assumed for pressures and 1 K for temperatures. Water vapour was assumed to have an uncertainty of 20 %, with 10 % for O_3 and HNO_3 and 5 % for CCl_4. The errors associated with the Gain, Shift and Spread were calculated using perturbations to the instrument line shape of 4 %, 2 % and 4 % respectively and an offset error of 2 nW/(cm^2 sr cm^{-1}) was assumed, with these values taken from Fischer et al. (2008). The error relating to the C_2H_2 spectroscopy was conservatively assumed to be 5 % with Jacquemart et al. (2003) giving an error of between 2 % and 5 %.

The total error on the retrieved VMR was estimated to be 15.6 % at 200 hPa, largely related to the random retrieval noise (14 %) and only 6.9 % related to the systematic errors. Of those systematic errors, the uncertainty in the C_2H_2 spectroscopy, instrument line-shape effects and pressure/temperature profiles were the dominant contributors; with only a minimal contribution from the uncertainty in the VMRs of other species in this spectral window. As the C_2H_2 profile decreases rapidly with altitude, above 120 hPa there is a greatly reduced signal and hence the random error increases substantially. At these high altitudes the O_3 and HNO_3 uncertainties add to the overall error whilst at lower altitudes (300 hPa and above), the uncertainty in water vapour VMR has a much larger affect.

3.4 Data evaluation

Unfortunately, there were very few measurements of C_2H_2 by other observing systems during the time period of the MIPAS nominal mode operations (full spectral resolution). The error analysis of the previous section provide the most reliable error characterisation of the data and the geophysical compactness of the relationships to CO (Sect. 4.1) indicate the quality of the data. However, comparisons to other data sets from different time periods provide a qualitative indication of the consistency of this MIPAS data set with other systems.

As identified in the recent work of González Abad et al. (2011), non-satellite data systems measuring C_2H_2 in the appropriate altitude ranges consist of MkIV balloon measurements and aircraft measurements from Trace-A (Fishman et al., 1996). Xiao et al. (2007) also present mean profiles for aircraft campaigns in the July–October timeframe: PEM-Tropics A and PEM-West A (Hoell et al., 1999) and INTEX-A (Singh et al., 2006).

The MkIV balloon measurements consist of five vertical profiles obtained in Septembers of 2003 to 2007 at Fort Sumner (34.4° N, 104.2° W). The most relevant data for September 2003 shows values between 45 and 55 ppt at 12 km, consistent with our monthly mean retrievals of 50 ppt in that region. The Trace-A data in late September and October 1992 sample a range of atmospheric regimes in the South Atlantic from biomass burning to clean air. González Abad et al. (2011) report mean values ranging between 80–120 ppt close to 12 km which are consistent with our mean values of 100 ppt for the region associated with the African biomass burning. However, such a comparison clearly depends on the intensity and extent of biomass burning in a given year. Similar considerations apply to PEM-Tropics A, PEM-West A and Intex-A for which the aircraft mean values are 50 ppt, 200 ppt, and 90 ppt (from Xiao et al., 2007) compared to 50, 130 and 80 ppt in the MIPAS retrievals.

Finally a preliminary assessment of our results was performed against the ACE-FTS research dataset used in Park et al. (2008). Unfortunately this comparison cannot be done for the same year and indeed the ACE-FTS data had to be averaged over all summer months (June–August) between 2004 and 2006. However, both the ACE-FTS data and the MIPAS data reported here observe a similar enhancement associated with the anticyclone, with values ranging from 65 ppt (ACE-FTS) compared to 60 ppt (MIPAS) outside the anticyclone to 150 ppt (ACE-FTS) compared to 200 ppt (MIPAS) within the core. Since the strength of the enhancement in the anticyclone is likely to vary as a function of yearly surface emissions, the differences within the core are very reasonable.

Hence, we conclude that the MIPAS retrievals of C_2H_2 in this paper are very consistent with literature values particularly in the areas with most likely lower interannual variability. The comparisons for higher concentrations of C_2H_2 are complicated by interannual source and transport variations

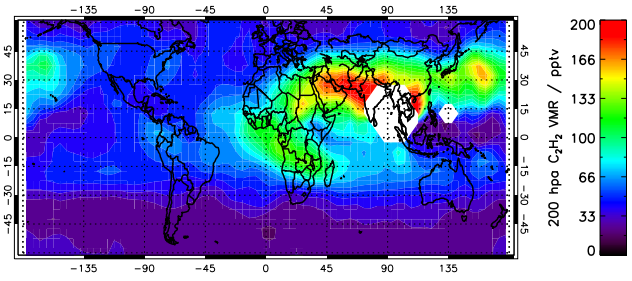

(a) 200 hpa C_2H_2

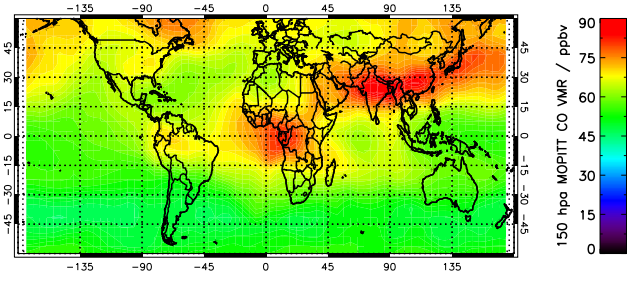

(b) 150 hpa MOPITT CO

Fig. 3. 200 hPa MORSE C_2H_2 VMRs and 150 hPa MOPITT CO VMRs averaged for August 2003. The strong chemical isolation related to the Asian monsoon anticyclone is the dominant feature but strong enhancements of both species are also observed relating to biomass burning in southern Africa and Asian outflow into the Pacific.

but are reasonable. Future comparisons with ACE-FTS data would be valuable but are not appropriate to this MIPAS data sets as it is confined to the nominal mode data obtained in 2003.

4 C_2H_2 retrieval results

4.1 Global behaviour

In the results that follow we concentrate on the 200 hPa level, at which the errors are smallest and random error dominates single profile retrievals.

Figure 3a shows all data for August 2003 at 200 hPa that pass the cloud and quality filters. The data are averaged onto a regular grid with a 5° resolution using a distance-weighted approach to calculate the mean; a scaling distance r of 10° from the grid box centre is used with a weighting of $1-x^2/r^2$, reaching zero at 10° from the box centre (i.e. at $x=r$). This method maintained the sharper gradients whilst producing a robust average of the individual observation values. Rather than introducing interpolation errors, the data are not interpolated vertically but instead an average pressure level is given, following the procedure of Moore and Remedios (2010).

A strong enhancement of C_2H_2 is observed over the Middle-Eastern region and clearly shows the enhanced C_2H_2 VMRs due to the Asian monsoon anticyclone as also reported by Park et al. (2008). Enhanced C_2H_2 mixing ratios are also observed over the African biomass burning region. The distributions in the most northerly latitudes, whilst greater than those in the corresponding southerly latitudes, are much lower in mixing ratio than in the African and Asian outflows.

4.2 C_2H_2 – CO relationships

The VMR of carbon monoxide is expected to be heavily correlated to that of C_2H_2 (Wang et al., 2004) with the C_2H_2/CO ratio an indicator of the relative age of the air mass and the extent of atmospheric processing it has undergone (Xiao et al., 2007; Smyth et al., 1996, 1999). In order to examine the C_2H_2 – CO relationship further, we use the 150 hPa MOPITT (Measurement Of Pollution In The Troposphere) Level 2 Version 3 data for the same time period. Maps of the concentrations of the two gases are shown in Fig. 3. It should be noted here that currently no suitably mature CO products are available for MIPAS itself, hence the use of MOPITT CO.

This comparison supports the interpretation that there is much in common between the two gases with respect to major inputs to the upper troposphere. However, there are also interesting differences. The C_2H_2 mixing ratios do not show strong features over Northern high latitudes and the Amazon unlike the CO data. In the Pacific region, the C_2H_2 provides a tighter definition of the local transport, close to Asia, rather than the CO which appears more even in VMR, indicating that C_2H_2 distributions may prove useful in further constraining particular transport pathways. These aspects indicate that C_2H_2 data could provide significant and complementary information to that contained in CO distributions.

Some care should be taken in interpreting detailed comparisons of the two data sets as whilst MIPAS is observing at a 12 km nominal altitude with an approximate 3 km field of view and a mean pressure of 200 hPa, MOPITT is a nadir-sounding instrument with the retrieved vertical levels a result of its broad averaging kernels in the troposphere. Typically the MOPITT CO 150 hPa averaging kernels have sensitivity between 400–100 hPa. We have estimated, by applying averaging kernels to typical profiles, that the effect of vertical resolution may lead to a systematic underestimation of the C_2H_2/CO ratio of approximately 10 % but that a strong correlation would still be expected between the relevant trace gas data from these two instruments.

The strong African biomass burning signature is clearly observed in both datasets, indicating that a C_2H_2 enhancement due to biomass burning is present. In addition, there are strong CO and C_2H_2 enhancements observed over Asia, particularly the extension of the monsoon anticyclone into the Northern Pacific accompanied by outflow to the North (see Figs. 3, 6 and 7) which is consistent with Bey et al. (2001)

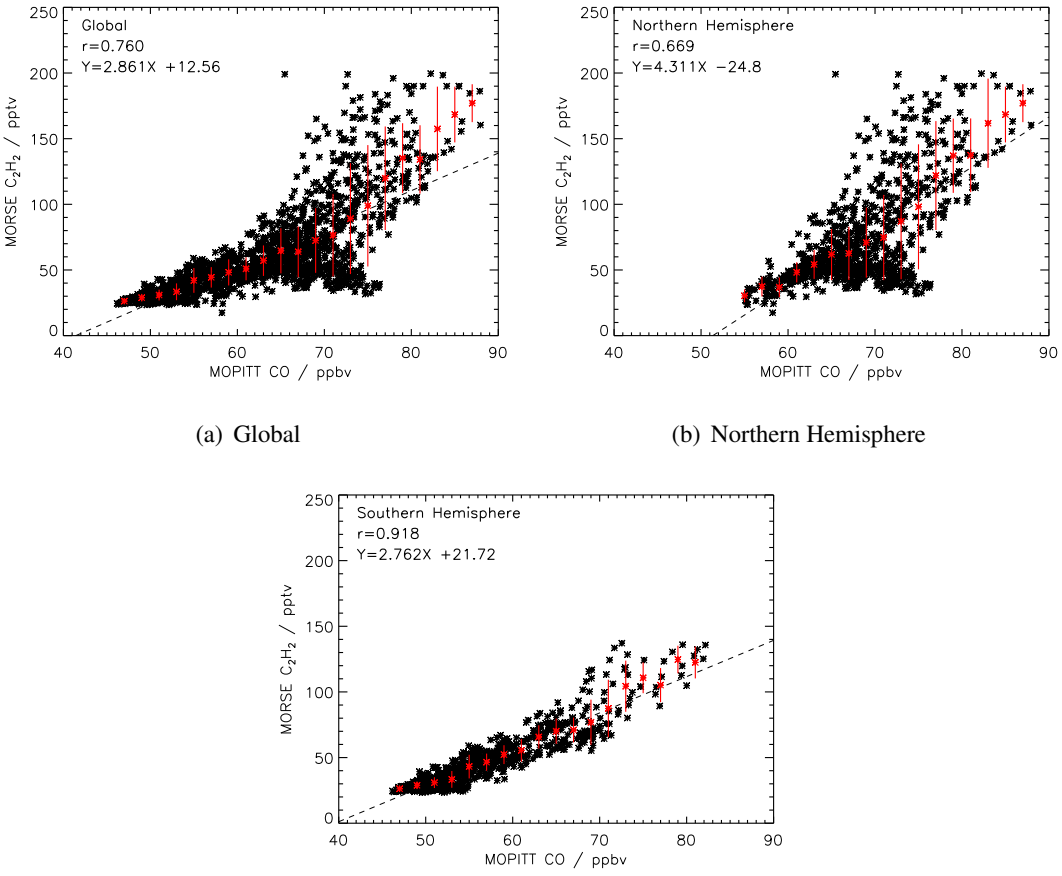

(a) Global

(b) Northern Hemisphere

(c) Southern Hemisphere

Fig. 4. Correlation of the 200 hPa MORSE C_2H_2 VMRs against 150 hPa MOPITT CO VMRs averaged for August 2003 for Globally, the Northern Hemisphere and the Southern Hemisphere. The two distinct domains observed in the global correlation are due to the differences in sources and transport for the Northern Hemisphere and Southern Hemisphere. The dashed lines indicate the line of best fit through the correlations. The red points show the average values in 2 ppbv bins, with the associated error bars indicating the standard deviation within each bin.

who state that the main export pathway for Asian pollution into the Pacific is the westerly flow north of 25°N. Although the data in the South-East Asia region is more sparse due to the cloud associated with the Asian monsoon, enhancements are observed over this region where data are present. It is the strong enhancement of both CO and C_2H_2 in the Middle East region which is of particular interest. Rather than surface production and vertical transport, the probable cause of this feature is long-range transport from the convective region over South-East Asia via the Easterly Jet associated with the Asian monsoon anticyclone into the Middle East. This is consistent with the discussion of a similar feature in Ozone observations by (Li et al., 2003).

The 200 hPa MORSE C_2H_2 VMRs were correlated against the 150 hPa MOPITT CO VMRs for the globally averaged monthly data and the result is shown in Fig. 4a with the red points indicating the mean values of the data along with their standard deviation, separated into 2 ppbv bins. This figure clearly shows a strong correlation between the two VMRs (with $r = 0.76$) but with two separate domains having distinctly different gradients.

The correlation was performed separately for the Northern (Fig. 4b) and Southern (Fig. 4c) Hemispheres and it is apparent that the two domains seen in the global correlation are due to the differences in C_2H_2 sources and transport between the two hemispheres. The strong correlation of 0.92 for the Southern Hemisphere is due to the relative lack of significant sources of C_2H_2 or long-range transport south of the equator. In contrast, the Northern Hemisphere contain the strong Asian C_2H_2 sources and a considerably higher background of CO resulting in a lower correlation of 0.67. The points with a low C_2H_2 values and high CO values are high latitude points where CO is enhanced but C_2H_2 is not.

The major biomass burning regions of Southern Africa (30° S to 10° N, 30° W to 80° E) and South America (30° S to 10° N, 180° W to 30° W) both show strong correlations, 0.81

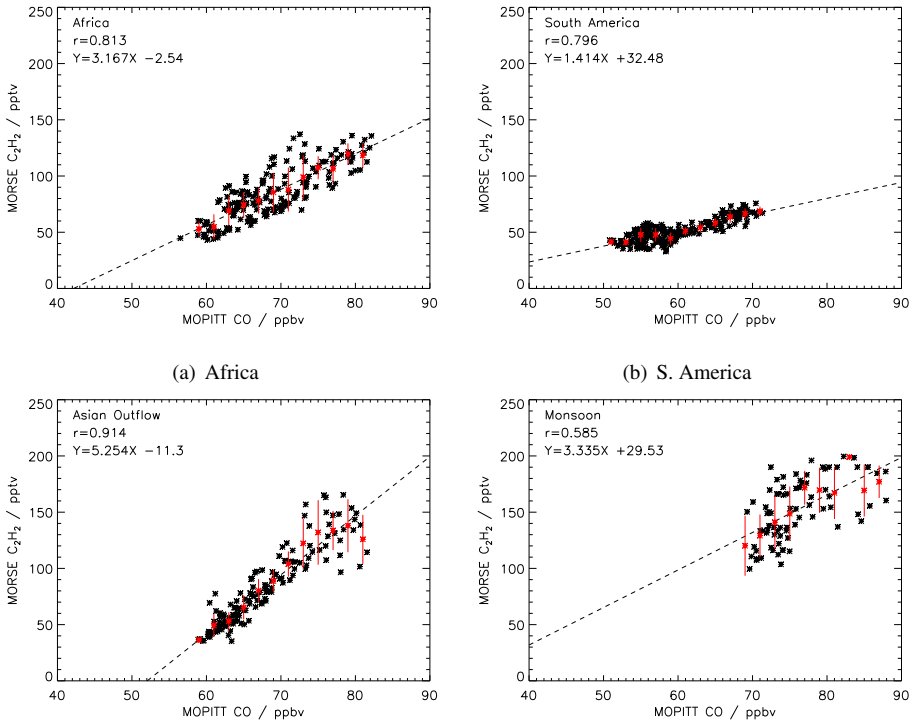

(a) Africa (b) S. America

(c) Asian Pacific (d) Monsoon

Fig. 5. 200 hPa MORSE C_2H_2 VMRs against 150 hPa MOPITT CO VMRs averaged for August 2003 for: Africa (30° S to 10° N, 30° W to 80° E), South America (30° S to 10° N, 180° W to 30° W), Asian Pacific Outflow (10° N to 40° N, 130° E to 110° W) and the Asian monsoon anticyclone region (10° N to 40° N, 30° E to 110° E). Again, the dashed lines indicate the line of best fit through the correlations. The red points show the average values in 2 ppbv bins, with the associated error bars indicating the standard deviation within each bin.

(Fig. 5a) and 0.80 (Fig. 5b) respectively. However, the regions are otherwise very different. The highest C_2H_2 VMRs of 150 pptv are observed directly over the African source region with the Amazon region showing much smaller C_2H_2 VMRS for the same CO mixing ratios. In the African sector, where significant transport into the Atlantic is observed, the gradient of the correlation is significantly higher (3.17) than in South America (1.41) indicating either very different source ratios of the two gases or a very different photochemical regime; dilution of the outflow plume would not show such an effect. It is interesting to note that the South American gradient is the smallest of the four regions studied here.

For the Asian outflow into the Pacific Ocean (10° N to 40° N, 130° E to 110° W), a correlation of 0.91 is observed (Fig. 5c) with a steep gradient (5.25). This strong correlation and steep gradient suggest that there is considerable transport between Asia and North America and that this occurs on a relatively short time-scale before the C_2H_2 has time to photochemically age.

Finally, the Asian monsoon anticyclone region (10° N to 40° N, 30° E to 110° E) has a correlation of 0.59 (Fig. 5d). Unlike the previous examples, the region here is largely isolated with convective injection toward the east (see Sect. 4.4). Although the correlation is reasonable, it appears that there is considerable variability in either ratios of C_2H_2 to CO sources or in the photochemical age of the observed C_2H_2.

Having illustrated that the C_2H_2 – CO relationship maintains strong correlations except in the strongest source regions where these are disturbed, it is instructive to examine the C_2H_2/CO ratio. Smyth et al. (1996) note that this ratio is preserved through the processes of convection and mixing. The gridded C_2H_2 and CO values (as shown in Fig. 3) are used to calculate the C_2H_2/CO ratio (Fig. 6). The highest ratios should be observed over source regions where C_2H_2 and CO are both produced from the combustion process and diminish with time as the photochemical age of air increases with atmospheric processing. Due to the difference in lifetimes of C_2H_2 (approximately 2 weeks) and CO (approximately 2 months), for a high C_2H_2/CO ratio to exist (i.e. greater than 2 pptv/ppbv, Smyth et al., 1996), the C_2H_2 must be relatively young and associated with recent combustion. The two most obvious regions are clearly the biomass burning and Asian monsoon anticyclone regions where the correlation relationships are disturbed.

Clear transport mechanisms can also be identified from the C_2H_2/CO ratio in Fig. 6. The high ratio located over

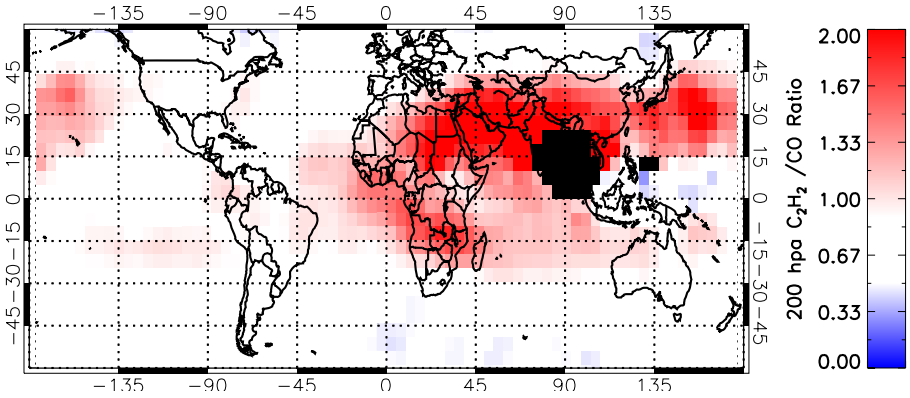

Fig. 6. 200 hPa MORSE C_2H_2/150 hPa MOPITT CO ratio for August 2003 calculated from the 5° globally gridded data (in units of pptv/ppbv). This ratio acts as an indicator of biomass burning sources and age of air and hence provides information on the relative speed of transport mechanisms. Features of note include the transport from African biomass into the Atlantic, transport from Asia into the Pacific and the isolation of the monsoon anticyclone.

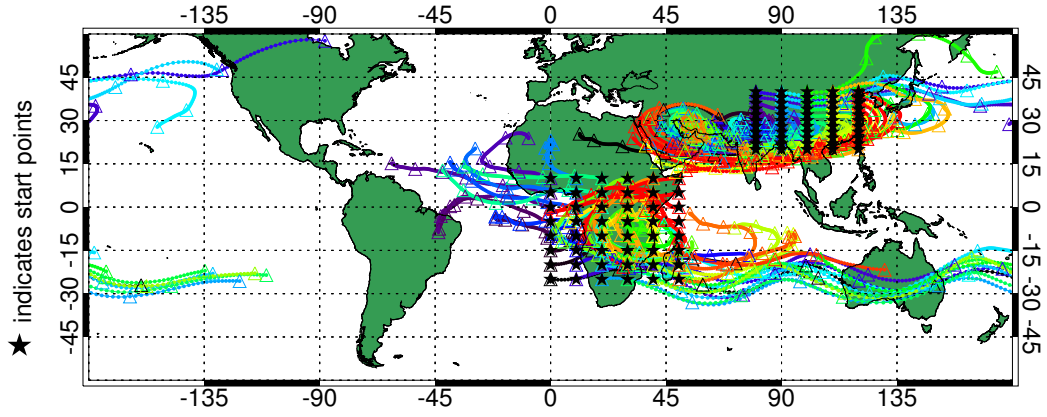

Fig. 7. Hysplit 5-day forward trajectories originating at a 12 km altitude over the Asian Monsoon anticyclone and the African biomass burning regions. The trajectory presented here was launched on 1st August but multiple trajectories were run for different start dates within August and found to be largely consistent in terms of the Asian monsoon anticyclone and global transport.

southern Africa is maintained as the African plume travels west out into the Atlantic Ocean. A further plume extends eastwards across Australia and towards South America, where the transportation can be seen much more clearly in the C_2H_2/CO ratio rather than in the CO field. A further transport pathway is observed from Asia into the Pacific Ocean and is related to the tongue of the Asian Monsoon anticyclone that extends over the Pacific (Bey et al., 2001) . This process is known to transport air relatively quickly, consistent with the observed high C_2H_2/CO ratio over the ocean where there are no source regions present. Figure 7 shows 5-day forward trajectory calculations performed using the HYSPLIT trajectory model and show a high consistency with the transport identified using the C_2H_2/CO ratio. These decay clearly along transport pathways where the 5-day trajectories indicate timescales for transport which are consistent with the spatial regions where the lower ratios are observed.

The fact that the C_2H_2/CO ratio is consistent with the known transport mechanisms in these regions provides confidence in the approach taken, allowing the transport from Asia into the Middle East to be discussed in the context of the C_2H_2/CO ratio. The high C_2H_2/CO ratio extends over the whole of the region and again clearly shows the strong chemical isolation of the monsoon. This is consistent with the behaviour of CO within the Asian monsoon anticyclone as observed from the Microwave Limb Sounder (MLS) by Li et al. (2005). Barret et al. (2010) goes on to show using assimilations of this data into the MOCAGE chemical transport model that South-East Asian pollution is uplifted into the upper troposphere and trapped within the Asian monsoon anticyclone where it is circulated over Northern Africa, behaving in the same way as the C_2H_2 isolation and transport observed here.

As this region is entirely over land some care must be taken to distinguish between a maintained high ratio due to

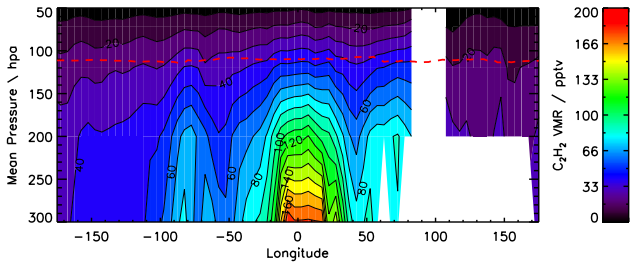

(a) East-West along 5 N

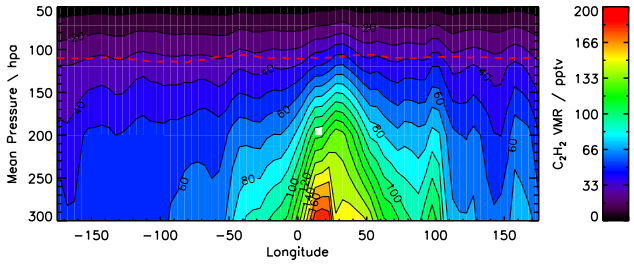

(b) East-West along 10 S

Fig. 8. Zonal cross-sections of the retrieved C_2H_2 distributions along the 5° N and 10° S lines of latitude, passing through the African biomass burning C_2H_2 enhancement. The NCEP mean tropopause pressure for August 2003 is shown by the red dashed line.

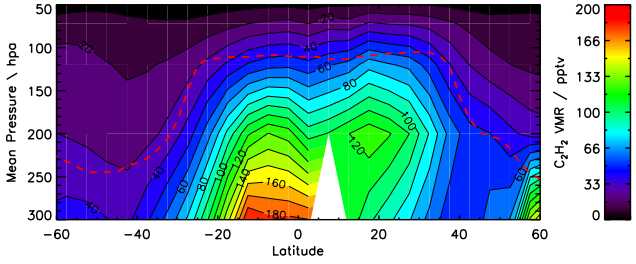

(a) North-South along 20 E

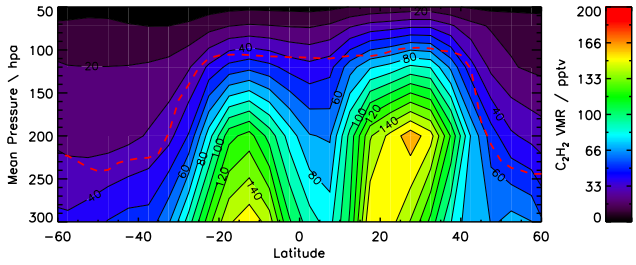

(b) North-South along 40 E

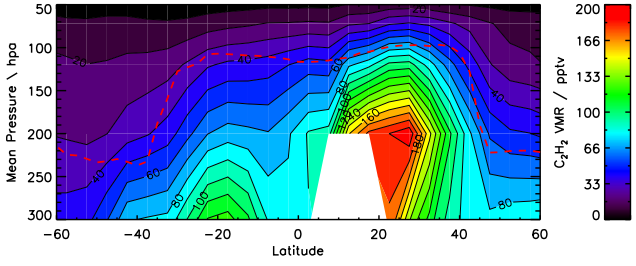

(c) North-South along 75 E

Fig. 9. Meridional cross-sections of the retrieved C_2H_2 distributions passing North-South through both the strong Asian monsoon anticyclone isolation and the African biomass burning enhancement at 20° E, 40° E and 75° E. The NCEP mean tropopause pressure for August 2003 is shown by the red dashed line.

fast transport or the alternative that the ratio remains high due to there being various combustion sources distributed over the whole region. There is no CO enhancement in the MOPITT lower levels in this region and the correlation for this region in the upper troposphere (Fig. 5d) remains relatively strong, albeit disturbed. Additionally, the fact that a clear gradient exists in the distribution of the high C_2H_2 and CO values (Fig. 3) between the Middle East and Northern Africa provides confidence that it is the Easterly Jet transport that is being observed. The anticyclone continues to transport newly formed C_2H_2 and CO into the region from the biomass and biofuel sources in Asia, leaving no time for substantial photochemical processing to occur before it is circulated back towards the source injection region at 200 hPa (see Sect. 4.4). It is this fast circulation due to the monsoon anticyclone which causes the persistence of the high C_2H_2/CO which is observed and also leads to the maximum observed at 170° E over the Pacific.

In the following sections we examine in more detail the C_2H_2 distributions relating to African biomass burning and the Asian monsoon anticyclone.

4.3 African biomass burning

In order to examine the C_2H_2 distributions in more detail, cross-sections have been plotted for both the zonal (Fig. 8) and meridional (Fig. 9) distributions. The NCEP mean tropopause pressure for August 2003 is shown as a red dashed line as a guide to the location of the troposphere and the stratosphere.

The C_2H_2 relating to African biomass burning is investigated through the use of zonal cross-sections taken along the 5° N and 10° S lines of latitude, passing through the African biomass burning C_2H_2 enhancement (Fig. 8). The cross-section along 5° N shows the biomass burning signal uplifted within the Inter-Tropical Convergence Zone (ITCZ) (Sauvage et al., 2007) but confined to below 250 hPa, well below the tropopause, with the outflow of C_2H_2 generally less than 100 pptv; this is consistent with Sauvage et al. (2005). The cross-section taken further south at 10° S shows a similar distribution but with the C_2H_2 extending higher into the atmosphere suggesting more intense biomass burning and a stronger uplift of C_2H_2 which is consistent with Barret et al. (2010) and Sauvage et al. (2007) who discuss the strong ascending winds in this region related to surface gradients in

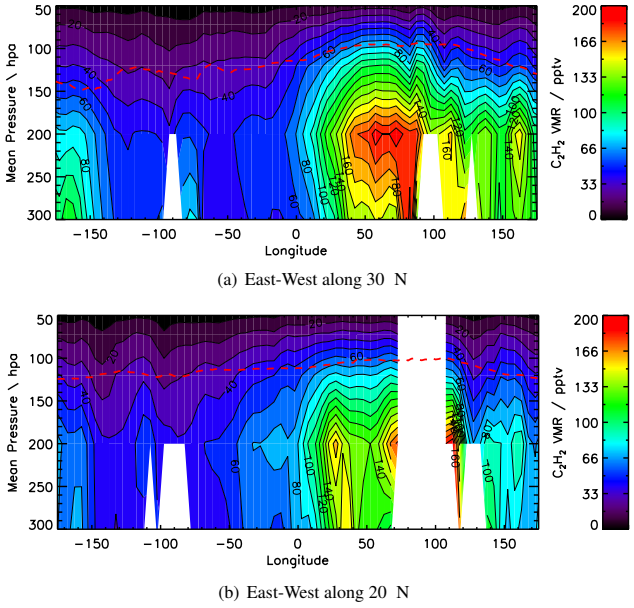

(a) East-West along 30 N

(b) East-West along 20 N

Fig. 10. Zonal cross-sections of the retrieved C_2H_2 distributions along the 20° N and 30° N lines of latitude, passing through the strong Asian monsoon anticyclone isolation. The NCEP mean tropopause pressure for August 2003 is shown by the red dashed line.

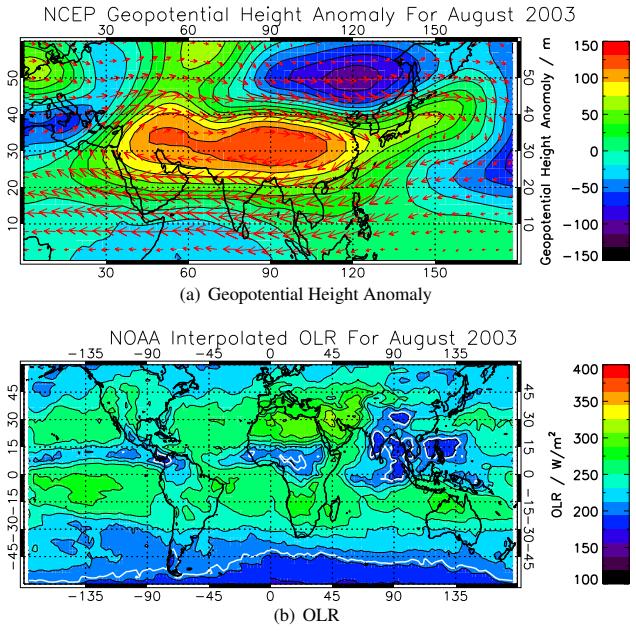

(a) Geopotential Height Anomaly

(b) OLR

Fig. 11. The Geopotential Height Anomaly and Outgoing Longwave Radiation for August 2003. The geopotential height anomaly is used as an indication for the anticyclone location and is shown to be in strong agreement with the enhanced C_2H_2 chemically isolated by the monsoon anticyclone. The OLR is used to indicate areas of deep convection (i.e. OLR $<205\,W\,m^{-2}$) which are outlined by the white contour lines. These show the large area of deep convection over India and South-East Asia, on the South-Eastern edge of the Asian monsoon anticyclone.

temperature and humidity. Outflow towards the east and west is also apparent with values above 100 pptv observed over both the Indian and Atlantic Oceans. Overall, the highest concentration of C_2H_2 at 250 hPa is found to be less than 150 ppt.

Meridional cross-sections of the C_2H_2 distribution were taken along the 20° E (Fig. 9a), 40° E (Fig. 9b) and 75° E (Fig. 9c) longitude lines, confirming these findings. Note that the cross-section at 20° E (Fig. 9a) includes the western edge of the anticyclone in the Northern Hemisphere and the African biomass burning region in the Southern Hemisphere. It is worth noting that there are apparently weak enhancements of C_2H_2 in the stratosphere above high values in the troposphere. Correlations suggest that these are a retrieval artefact and no other evidence of enhanced stratospheric values could be observed. This subject is returned to in the next section.

4.4 The Asian monsoon anticyclone

In contrast to Africa, the strong C_2H_2 enhancement in the Asian monsoon anticyclone is observed as high as 150 hPa, reaching the tropopause inside the core of the anti-cyclone at 75° E (Fig. 9c). Values of at least 200 ppt are observed. This suggests that the observed uplift from the monsoon convection is considerably stronger or occurs on a faster timescale compared to the weaker convection observed over Africa. The meridional distributions and outgoing longwave radiation (OLR) show that the main monsoon convection is occurring between 0 and 20° N, with some convection extending further north. The data show very clearly that the C_2H_2 mixing ratios are very strongly related to the convective systems (marked by the OLR; also by the white areas of cloud in Fig. 10 and 12). Following injection, the enhancement moves northwards and westwards from the convective region into the centre of the anticyclone at 200 hPa. This is consistent with the work of Park et al. (2007) who note a clear distinction between the location of the anticyclone circulation and the convective region over India and South-East Asia coupled through convective outflow into the anticyclone at this altitude. The 150 hPa geopotential height anomaly calculated from NCEP meteorological data (Fig. 11a) shows the position of the Asian monsoon anti-cyclone and the associated wind field for this month and again is highly consistent with the C_2H_2 distributions.

Zonal cross-sections of C_2H_2 were taken along the 20° N and 30° N latitude lines passing through the strong Asian monsoon anticyclone isolation. The cross-section taken across the centre of the anticyclone core at 30° N (Fig. 10a) shows the extent of the chemical isolation with a strong gradient both across the western edge of the anticyclone and vertically as the C_2H_2 is constrained beneath the tropopause.

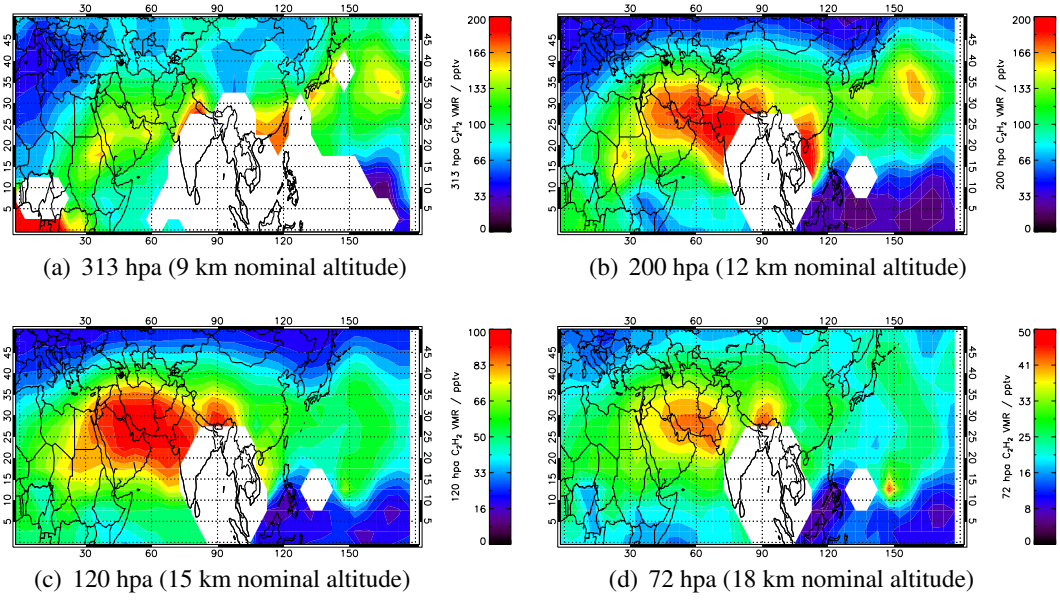

(a) 313 hpa (9 km nominal altitude) (b) 200 hpa (12 km nominal altitude)

(c) 120 hpa (15 km nominal altitude) (d) 72 hpa (18 km nominal altitude)

Fig. 12. The MORSE retrieved C_2H_2 distributions for August 2003 located over the Asian monsoon anticyclone region for the 9 km, 12 km, 15 km and 18 km nominal MIPAS tangent altitudes. The strong Asian monsoon anticyclone isolation is clearly evident as well as significant transport from Asia towards North America, particulary at lower altitudes.

The dramatic change in the C_2H_2 profiles across the monsoon boundary show the strength of the chemical isolation inside the monsoon as previously identified by Park et al. (2008) but with much higher spatial and temporal resolution. The zonal cross-section at 20° N (Fig. 10b) transects the convective region of the monsoon located over India and South-East Asia as indicated by OLR values less than 205 W m^{-2} (Fig. 11b). Although the centre of the convective region contains no cloud-free data, the enhancements observed on the edge of this region support the conclusion that the C_2H_2 is uplifted from within this convective region. Additionally, the zonal cross-section at 30° N (Fig. 10a) shows the eastward transport of enhanced VMRs at 200 hPa into the Asian-Pacific.

Figure 12 shows the C_2H_2 distributions at the four MIPAS levels with average pressures of 313, 200, 120 and 72 hPa (the 9, 12, 15 and 18 km nominal altitudes). Figure 12b illustrates the convection-related uplift, the distinct gradients maintained around the core of the anti-cyclone and the enhancement of the VMRs in the core. At 120 hPa, the dominant feature is displaced eastwards from South-East Asia and India, consistent with the time-averaged, June–August HCN distributions from ACE reported by Randel et al. (2010). In addition, one can observe a strong eastward extension of the anticyclone which results in high mixing ratios in an apparent maximum near 170° E in the region where troposphere-stratosphere exchange may be expected to occur (Lelieveld et al., 2002). Hence the fate of the air in this extension is an important consideration for future studies. Such a feature over the Pacific could clearly be mis-interpreted in nadir sounding data emphasising the complementarity of good limb sounding observations.

A set of typical averaging kernels for these C_2H_2 MIPAS retrievals over the monsoon anticyclone region are shown in Fig. 13 and clearly show strong peaks at approximately 300 hPa, 200 hPa and 120 hPa. The C_2H_2 response function above 120 hPa shows that these data are highly reflective of the 120 hPa level itself and so should be highly correlated with it. Our data reflect this in both global and local correlations (not shown). Therefore in our data, we cannot assert that the distributions at 72 hPa unambiguously reflect stratospheric enhancements where they overlie enhanced VMRs in the troposphere below it. This is an important but subtle point. Randel et al (2010) and references therein note that upward circulation on the eastern side of the anticyclone results in transport into the stratosphere and our data is consistent with this. However, it is very difficult to distinguish the data effects from the transport effects and the vertical correlations in our retrievals suggest that interpretation of this feature at least in our MIPAS data set requires considerable care. Secondly, it suggests that the potential for upward circulation across the different parts of the anticyclone remains difficult to observe and further observations are necessary, particularly to the west of the convective region.

5 Conclusions

Mixing ratios of C_2H_2 has been successfully retrieved from MIPAS spectral radiances for August 2003 when the instrument was operating in nominal mode at the highest spectral

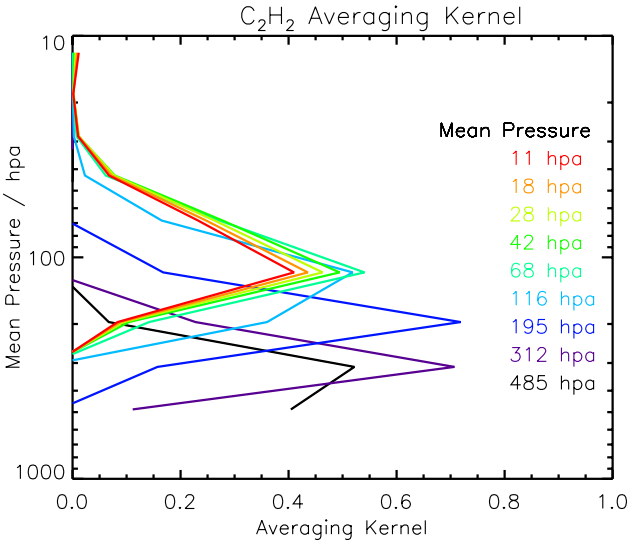

Fig. 13. A example of a typical averaging kernel over the monsoon anticyclone showing the sensitivity of the retrieval at 200 hPa and 300 hPa. Note that there is no discernible C_2H_2 signal above 100 hPa as expected, the C_2H_2 sensitivity is largely confined to the upper troposphere.

resolution. Between 300 hPa and 100 hPa, estimated systematic errors are 15 % at best with random errors between 15 %, 10 % and 30 %. Evaluation of the data indicates reasonable agreement with literature values, albeit limited by the lack of space-time coincidence with other observing systems. As a result of the good data quality, we have been able to produce the first global maps of C_2H_2 and ratios to CO, providing a key indicator of surface source injection into the upper troposphere, transport and decay due to photochemistry and dilution. Strong signatures are clearly evident and are associated with chemical isolation in the Asian monsoon anticyclone and with the export of African biomass burning.

The C_2H_2 VMR has been used in conjunction with the 150 hPa MOPITT CO VMR to examine the correlation between C_2H_2 and CO. When performed globally, these calculations showed a strong correlation between the C_2H_2 and CO of 0.76 but with two distinct domains due to the Northern and Southern Hemispheres. When correlated individually, the Northern Hemisphere had a correlation of 0.67 showing the much greater variability in the transport and sources compared to the Southern Hemisphere whose correlation was 0.918 but with significantly lower C_2H_2 values. Defining the geographical regions to limit the influence of the variability from different sources allowed stronger correlations to be revealed. Africa, South America, and the Asian Pacific outflow regions all correlated strongly. Even for the case over the Middle East/Asia where these is no clear ocean background influence to distinguish the enhancements from, a reasonable correlation between C_2H_2 and CO still existed.

As the C_2H_2 and CO remain well correlated through transport and mixing, this allowed the C_2H_2/CO ratio to be calculated and analysed as a marker of source injection regions and subsequent photochemical ageing in the outflow regions. A strong C_2H_2 signal was retrieved over the Middle East region and the C_2H_2/CO ratio allowed us to observe enhanced C_2H_2 concentrations resulting from the fast outflow from Asia associated with the monsoon anticyclone. This enhancement was maintained by the influence of the anticyclone associated with the monsoon, which acts as a barrier to further transport, and by the fast re-circulation time within the anticyclone.

African biomass burning was characterised by more regionally strong emissions leading to outflows away from the continent. Our data suggest that transport regimes from Southern Africa into the Atlantic/Indian Oceans and the transport from Asia into the Pacific Ocean are well-defined in the C_2H_2 fields, and better marked in the upper troposphere than the CO. The C_2H_2/CO ratio appears to decay strongly along these known pathways, probably due to photochemical ageing, and results in the C_2H_2 appearing to be more tightly confined along the transport pathways compared to the CO which due to its longer lifetime may be more governed by dilution. The timescale of the outflow effects was verified through the use of 5 day trajectory modelling which provided further confidence in both the C_2H_2 retrieval and in the use of the C_2H_2/CO ratio as an indicator for the photochemical age of air in future work.

By examining cross-sections through the anticyclone, the horizontal and vertical extent of the isolation was shown. The location of the convective region over India and South-East Asia as identified by OLR data was also evident from these cross-sections, strongly suggesting that it is from this region where the C_2H_2 is delivered into the upper troposphere at fast timescales, followed by advection at 200 hPa. Analysis of the geopotential height anomaly and 150 hPa wind vectors were also used to verify the location of the C_2H_2 within the anticyclone. The build-up of C_2H_2 in the eastward extension of the anticyclone was also remarkable and allows for comparisons to model studies of this isolation. The current MIPAS dataset is consistent with upward circulation on the eastern side of the anticyclone but cannot unambiguously identify transportation into the lower stratosphere anywhere in the anticyclone due to vertical correlations.

A similar analysis was performed for the African biomass burning enhancements. Here the uplift was observed not to penetrate as high into the troposphere as for the Asian monsoon anticyclone and to be more dominated by outflow. C_2H_2 mixing ratios at 250 hPa were less than 150 ppt in contrast to 200 ppt or more within the anticyclone.

In summary, we have shown that is is possible to use MIPAS data to explore the upper-tropospheric distributions of C_2H_2 with a much higher temporal and spatial resolution than has previously been possible. The ratio of C_2H_2-CO was shown to provide information on the injection of surface

emissions and transport of photochemically aged plumes. In addition, we have shown that MIPAS C_2H_2 can act as a tracer for investigating dynamical effects such as convective regions for trace gases, advection, outflow and long-range transport. Due to the high spatial sampling, this data would prove suitable for further exploitation by comparisons to modelled data in order to study these effects further. We therefore believe that where possible, routine retrieval of these species in the future would be highly desirable.

Ideally it would be possible to compare MIPAS C_2H_2 data sets with other direct observations, although MIPAS data sets for other trace species are well characterised and compare well with other species. In the future, it would be possible to develop a retrieval for the MIPAS optimised mode (lower spectral resolution) and enable a direct comparison with ACE-FTS data sets which also lack data sets for intercomparison. This would further support the excellent advances in global observations of organics species in the troposphere that have been made in the last ten years.

Acknowledgements. Robert Parker was supported by a research studentship from the Natural Environment Research Council. David Moore was supported by the National Centre For Earth Observation (NCEO). Vijay Kanawade was supported from SPARTAN project contract number MEST-CT-2004-7512. The authors wish to thank the European Space Agency for access to MIPAS data under CUTLSOM (AO-357). The MOPITT Level 2 (L2) Version 3 data used in this study was obtained from the NASA Langley Research Center Atmospheric Science Data Center. We would also like to thank Anu Dudhia for providing us with the Oxford Reference Forward Model (RFM) and the MIPAS Orbital Retrieval using Sequential Estimation (MORSE) code used in this study. The authors also gratefully acknowledge the NOAA Air Resources Laboratory (ARL) for the provision of the HYSPLIT transport and dispersion model used in this publication.

Edited by: B. N. Duncan

References

Barret, B., Williams, J. E., Bouarar, I., Yang, X., Josse, B., Law, K., Pham, M., Le Flochmoën, E., Liousse, C., Peuch, V. H., Carver, G. D., Pyle, J. A., Sauvage, B., van Velthoven, P., Schlager, H., Mari, C., and Cammas, J.-P.: Impact of West African Monsoon convective transport and lightning NOx production upon the upper tropospheric composition: a multi-model study, Atmos. Chem. Phys., 10, 5719–5738, doi:10.5194/acp-10-5719-2010, 2010.

Bernath, P. F., McElroy, C. T., Abrams, M. C., Boone, C. D., Butler, M., Camy-Peyret, C., Carleer, M., Clerbaux, C., Coheur, P., Colin, R., DeCola, P., DeMazire, M., Drummond, J. R., Dufour, D., Evans, W. F. J., Fast, H., Fussen, D., Gilbert, K., Jennings, D. E., Llewellyn, E. J., Lowe, R. P., Mahieu, E., McConnell, J. C., McHugh, M., McLeod, S. D., Michaud, R., Midwinter, C., Nassar, R., Nichitiu, F., Nowlan, C., Rinsland, C. P., Rochon, Y. J., Rowlands, N., Semeniuk, K., Simon, P., Skelton, R., Sloan, J. J., Soucy, M., Strong, K., Tremblay, P., Turnbull, D., Walker, K. A., Walkty, I., Wardle, D. A., Wehrle, V., Zander, R., and Zou, J.: Atmospheric chemistry experiment (ACE): Mission overview, Geophys. Res. Lett., 32, L15S01, doi:10.1029/2005GL022386, 2005.

Bertschi, I. T., Yokelson, R. J., Ward, D. E., Christian, T. J., and Hao, W. M.: Trace gas emissions from the production and use of domestic biofuels in Zambia measured by open-path Fourier transform infrared spectroscopy, J. Geophys. Res. Atmos., 108, 8469, doi:10.1029/2002JD002158, 2003.

Bey,I., Jacob,D. J., Logan,J. A., Yantosca,R. M.: Asian chemical outflow to the Pacific in spring: Origins, pathways, and budgets, J. Geophys. Res. Atmos., 106, 23097–23113, 2001.

Blake, N. J., Blake, D. R., Sive, B. C., Chen, T. Y., Rowland, F. S., Collins Jr, J. E., Sachse, G. W., and Anderson, B. E.: Biomass burning emissions and vertical distribution of atmospheric methyl halides and other reduced carbon gases in the South Atlantic region, J. Geophys. Res. Atmos., 101, 24151–24164, 1996.

Dudhia, A.: MIPAS Orbital Retrieval using Sequential Estimation, available online at: http://www.atm.ox.ac.uk/MORSE/, 2005a.

Dudhia, A.: The Oxford Reference Forward Model, available online at: http://www.atm.ox.ac.uk/RFM/, 2005b.

Edwards, D. P.: GENLN2: A general line-by-line atmospheric transmittance and radiance model. Version 3.0: Description and users guide, Report NCAR/TN-367 +STR, National Center for Atmospheric Research, Boulder, Colorade, USA, 1992.

Fischer, H., Birk, M., Blom, C., Carli, B., Carlotti, M., von Clarmann, T., Delbouille, L., Dudhia, A., Ehhalt, D., Endemann, M., Flaud, J. M., Gessner, R., Kleinert, A., Koopman, R., Langen, J., López-Puertas, M., Mosner, P., Nett, H., Oelhaf, H., Perron, G., Remedios, J., Ridolfi, M., Stiller, G., and Zander, R.: MIPAS: an instrument for atmospheric and climate research, Atmos. Chem. Phys., 8, 2151–2188, doi:10.5194/acp-8-2151-2008, 2008.

Fishman, J., Hoell, J. M., Bendura, R. D., McNeal, R. J., and Kirchhoff, V. W. J. H: NASA GTE TRACE A Experiment (September–October 1992): Overview, J. Geophys. Res., 101(D19), 23865–23879, 1996.

Glatthor, N., von Clarmann, T., Fischer, H., Funke, B., Grabowski, U., Höpfner, M., Kellmann, S., Kiefer, M., Linden, A., Milz, M., Steck, T., and Stiller, G. P.: Global peroxyacetyl nitrate (PAN) retrieval in the upper troposphere from limb emission spectra of the Michelson Interferometer for Passive Atmospheric Sounding (MIPAS), Atmos. Chem. Phys., 7, 2775–2787, doi:10.5194/acp-7-2775-2007, 2007.

González Abad, G. , Allen, N. D. C. , Bernath, P. F. , Boone, C. D., McLeod, S. D. , Manney, G. L. , Toon, G. C., Carouge, C., Wang, Y., Wu, S., Barkley, M. P., Palmer, P. I., Xiao, Y. and Fu, T. M: Ethane, ethyne and carbon monoxide concentrations in the upper troposphere and lower stratosphere from ACE and GEOS-Chem: a comparison study, Atmos. Chem. Phys., 11, 9927–9941, doi:10.5194/acp-11-9927-2011, 2011.

Hegg, D. A., Radke, L. F., Hobbs, P. V., Rasmussen, R. A., and Riggan, P. J.: Emissions of some trace gases from biomass fires, J. Geophys. Res., 95, 5669–5675, 1990.

Hoell, J. M., Davis, D. D., Jacob, D. J., Rodgers, M. O., Newell, R. E., Fuelberg, H. E., McNeal, R. J., Raper, J. L., and Bendura, R. J.: Pacific Exploratory Mission in the tropical Pacific: PEM-Tropics A, August–September 1996, J. Geophys. Res. Atmos.,

104, 5567–5583, 1999.

Jacquemart, D., Mandin, J. Y., Dana, V., Claveau, C., Vander Auwera, J., Herman, M., Rothman, L., Regalia-Jarlot, L., and Barbe, A.: The IR acetylene spectrum in HITRAN: update and new results, J. Quant. Spectrosc. Rad., 82, 363–382, 2003.

Li, Q., Jacob, D. J., Logan, J. A., Bey, I., Yantosca, R. M., Liu, H., Martin, R. V., Fiore, A. M., Field, B. D., Duncan, B. N., Thouret, V.:A tropospheric ozone maximum over the Middle East, Geophys. Res. Lett., 28, 17, 3235–3238, 2001.

Li, Q., Jiang, J. H., Wu, D. L., Read, W. G. , Livesey, N. J., Waters, J. W., Zhang, Y., Wang, B., Filipiak, M. J., Davis,C. P., Turquety,S., Wu,S., Park,R. J., Yantosca,R. M., Jacob,D. J.: Convective outflow of South Asian pollution: A global CTM simulation compared with EOS MLS observations, Geophys. Res. Lett., 32, 1–4, 2005.

Lelieveld, J., Berresheim, H., Borrmann, S., Crutzen, P. J, Dentener, F. J, Fischer, H., Feichter, J., Flatau,P. J., Heland,J., Holzinger,R., Korrmann,R., Lawrence,M. G., Levin,Z., Markowicz,K. M., Mihalopoulos N., Minikin,A., Ramanathan,V., De Reus,M., Roelofs,G. J., Scheeren,H. A., Sciare,J., Schlager,H., Schultz,M., Siegmund,P., Steil,B., Stephanou,E. G., Stier,P., Traub,M., Warneke,C., Williams,J. and Ziereis,H:Global air pollution crossroads over the Mediterranean, Science, 298, 5594, 794–799, 2002.

Moore, D. P. and Remedios, J. J.: Growth rates of stratospheric HCFC-22, Atmos. Chem. Phys., 8, 73–82, doi:10.5194/acp-8-73-2008, 2008.

Moore, D. P. and Remedios, J. J.: Seasonality of Peroxyacetyl nitrate (PAN) in the upper troposphere and lower stratosphere using the MIPAS-E instrument, Atmos. Chem. Phys., 10, 6117–6128, doi:10.5194/acp-10-6117-2010, 2010.

Park, M., Randel, W. J., Gettelman, A., Massie, S. T., and Jiang, J. H.: Transport above the Asian summer monsoon anticyclone inferred from Aura Microwave Limb Sounder tracers, J. Geophys. Res. Atmos., 112, D16309, doi:10.1029/2006JD008294, 2007.

Park, M., Randel, W. J., Emmons, L. K., Bernath, P. F., Walker, K. A., and Boone, C. D.: Chemical isolation in the Asian monsoon anticyclone observed in Atmospheric Chemistry Experiment (ACE-FTS) data, Atmos. Chem. Phys., 8, 757–764, doi:10.5194/acp-8-757-2008, 2008.

Randel, W. J., Park, M., Emmons, L., Kinnison, D., Bernath, P., Walker, K. A., Boone, C., and Pumphrey, H.: Asian monsoon transport of pollution to the stratosphere, Science, 328, 611–613, 2010.

Raspollini, P., Belotti, C., Burgess, A., Carli, B., Carlotti, M., Ceccherini, S., Dinelli, B. M., Dudhia, A., Flaud, J.-M., Funke, B., Höpfner, M., López-Puertas, M., Payne, V., Piccolo, C., Remedios, J. J., Ridolfi, M., and Spang, R.: MIPAS level 2 operational analysis, Atmos. Chem. Phys., 6, 5605–5630, doi:10.5194/acp-6-5605-2006, 2006.

Remedios, J. J., Allen, G., Waterfall, A. M., Oelhaf, H., Kleinert, A., and Moore, D. P.: Detection of organic compound signatures in infra-red, limb emission spectra observed by the MIPAS-B2 balloon instrument, Atmos. Chem. Phys., 7, 1599–1613, doi:10.5194/acp-7-1599-2007, 2007.

Rinsland, C. P., Gunson, M. R., Wang, P. H., Arduini, R. F., Baum, B. A., Minnis, P., Goldman, A., Abrams, M. C., Zander, R., Mahieu, E., Salawitch, R. J., Michelsen, H. A., Irion, F. W., and Newchurch, M. J.: ATMOS/ATLAS 3 infrared profile measurements of trace gases in the November 1994 tropical and subtropical upper troposphere, J. Quant. Spectrosc. Ra., 60, 891–901, 1998.

Rinsland, C. P., Dufour, G., Boone, C. D., Bernath, P. F., and Chiou, L.: Atmospheric Chemistry Experiment (ACE) measurements of elevated Southern Hemisphere upper tropospheric CO, C_2H_6, HCN, and C_2H_2 mixing ratios from biomass burning emissions and long-range transport, Geophys. Res. Lett., 32, 1–4, 2005.

Rodgers, C.: Inverse methods for atmospheric sounding: theory and practice, World Scientific, 2000.

Rothman, L. S., Jacquemart, D., Barbe, A., Benner, D. C., Birk, M., Brown, L. R., Carleer, M. R., Chackerian Jr., C., Chance, K., Coudert, L. H., Dana, V., Devi, V. M., Flaud, J. ., Gamache, R. R., Goldman, A., Hartmann, J. ., Jucks, K. W., Maki, A. G., Mandin, J. ., Massie, S. T., Orphal, J., Perrin, A., Rinsland, C. P., Smith, M. A. H., Tennyson, J., Tolchenov, R. N., Toth, R. A., Vander Auwera, J., Varanasi, P., and Wagner, G.: The HITRAN 2004 molecular spectroscopic database, J. Quant. Spectrosc. Ra., 96, 139–204, 2005.

Sauvage, B., Thouret, V., Cammas, J. P., Gheusi, F., Athier, G. and Nedelec, P.:Tropospheric ozone over Equatorial Africa: regional aspects from the MOZAIC data, Atmos. Chem. Phys., 5, 311–335, 2005.

Sauvage, B., Gheusi, F., Thouret, V., Cammas, J.-P., Duron, J., Escobar, J., Mari, C., Mascart, P., and Pont, V.: Medium-range mid-tropospheric transport of ozone and precursors over Africa: two numerical case studies in dry and wet seasons, Atmos. Chem. Phys., 7, 5357–5370, doi:10.5194/acp-7-5357-2007, 2007.

Singh, H. B., Brune, W. H., Crawford, J. H., Jacob, D. J., and Russell, P. B.:Overview of the summer 2004 Intercontinental Chemical Transport Experiment-North America (INTEX-A), J. Geophys. Res. Atmos., 111, 24, doi:10.1029/2006JD007905, 2006.

Smyth, S. B., Sandholm, S. T., Bradshaw, J. D., Talbot, R. W., Blake, D. R., Blake, N. J., Rowland, F. S., Singh, H. B., Gregory, G. L., Anderson, B. E., Sachse, G. W., Collins, J. E., and Bachmeier, A. S.: Factors influencing the upper free tropospheric distribution of reactive nitrogen over the South Atlantic during the TRACE A experiment, J. Geophys. Res. Atmos., 101, 24165–24186, 1996.

Smyth, S., Sandholm, S., Shumaker, B., Mitch, W., Kanvinde, A., Bradshaw, J., Liu, S., McKeen, S., Gregory, G., Anderson, B., Talbot, R., Blake, D., Rowland, S., Browell, E., Fenn, M., Merrill, J., Bachmeier, S., Sachse, G., and Collins, J.: Characterization of the chemical signatures of air masses observed during the PEM experiments over the western Pacific, J. Geophys. Res. Atmos., 104, 16243–16254, 1999.

Spang, R., Remedios, J. J., and Barkley, M. P.: Colour indices for the detection and differentiation of cloud types in infra-red limb emission spectra, Adv. Space Res., 33, 1041–1047, 2004.

Streets, D. G., Bond, T. C., Carmichael, G. R., Fernandes, S. D., Fu, Q., He, D., Klimont, Z., Nelson, S. M., Tsai, N. Y., Wang, M. Q., Woo, J. H., and Yarber, K. F.: An inventory of gaseous and primary aerosol emissions in Asia in the year 2000, J. Geophys. Res. Atmos., 108, 8809, doi:10.1029/2002JD003093, 2003.

Talbot, R., Dibb, J., Scheuer, E., Seid, G., Russo, R., Sandholm, S., Tan, D., Singh, H., Blake, D., Blake, N., Atlas, E., Sachse, G., Jordan, C., and Avery, M.: Reactive nitrogen in Asian continental outflow over the western Pacific: Results from

the NASA Transport and Chemical Evolution over the Pacific (TRACE-P) airborne mission, J. Geophys. Res. Atmos., 108, 8803, doi:10.1029/2002JD003129, 2003.

Volkamer, R., Ziemann, P. J., and Molina, M. J.: Secondary Organic Aerosol Formation from Acetylene (C_2H_2): seed effect on SOA yields due to organic photochemistry in the aerosol aqueous phase, Atmos. Chem. Phys., 9, 1907–1928, doi:10.5194/acp-9-1907-2009, 2009.

von Clarmann, T., Glatthor, N., Koukouli, M. E., Stiller, G. P., Funke, B., Grabowski, U., Höpfner, M., Kellmann, S., Linden, A., Milz, M., Steck, T., and Fischer, H.: MIPAS measurements of upper tropospheric C_2H_6 and O_3 during the southern hemispheric biomass burning season in 2003, Atmos. Chem. Phys., 7, 5861–5872, doi:10.5194/acp-7-5861-2007, 2007.

Wang, T., Wong, C. H., Cheung, T. F., Blake, D. R., Arimoto, R., Baumann, K., Tang, J., Ding, G. A., Yu, X. M., Li, Y. S., Streets, D. G., and Simpson, I. J.: Relationships of trace gases and aerosols and the emission characteristics at Lin'an, a rural site in eastern China, during spring 2001, J. Geophys. Res. Atmos., 109, D19S05, doi:10.1029/2003JD004119, 2004.

Whitby, R. A. and Altwicker, E. R.: Acetylene in the atmosphere: sources, representative ambient concentrations and ratios to other hydrocarbons, Atmos. Environ., 12, 1289–1296, 1978.

Xiao, Y., Jacob, D. J., and Turquety, S.: Atmospheric acetylene and its relationship with CO as an indicator of air mass age, J. Geophys. Res. Atmos., 112, D12305, doi:10.1029/2006JD008268, 2007.